

**REPORT DOCUMENTATION PAGE**

Public reporting burden for this collection of information is estimated to average 1 hour per response, including the time for reviewing the data needed, and completing and reviewing this collection of information. Send comments regarding this burden estimate or reducing this burden to Washington Headquarters Services, Directorate for Information Operations and Reports, 1215 Jefferson Management and Budget, Paperwork Reduction Project (0704-0188), Washington, DC 20503

<b>1. AGENCY USE ONLY (Leave blank)</b>		<b>2. REPORT DATE</b> 2/28/2006	<b>3. REPORT TYPE AND DATES COVERED</b> Final Report: 4/1/06 to 11/31/06
<b>4. TITLE AND SUBTITLE</b> Active Control of Transverse Jets For Film Cooling Applications: A limited statement of work			<b>5. FUNDING NUMBERS</b> FA9550-05-1-0219
<b>6. AUTHOR(S)</b> D. E. Nikitopoulos			
<b>7. PERFORMING ORGANIZATION NAME(S) AND ADDRESS(ES)</b> D. E. Nikitopoulos Center for Turbine Innovation and Energy Research Mechanical Engineering Dept. Louisiana State University Baton Rouge, LA 70803			<b>8. PERFORMING ORGANIZATION REPORT NUMBER</b>
<b>9. SPONSORING / MONITORING AGENCY NAME(S) AND ADDRESS(ES)</b> Rhett Jefferies, Lt Col, USAF AFOSR, Turbulence and Rotating Flows Program Aerospace and Materials Sciences Directorate 875 North Randolph Street, Suite 325, Room 3112 Arlington, VA 22203-1768			<b>10. SPONSORING / MONITORING AGENCY REPORT NUMBER</b>

**11. SUPPLEMENTARY NOTES**

**12a. DISTRIBUTION / AVAILABILITY STATEMENT**

Approved for public release, distribution unlimited

**20060614011**

**13. ABSTRACT (Maximum 200 Words)**  
The objective of this project was to initiate investigation of film cooling flow control in order to improve its performance through active excitation of the film-cooling jet. A theoretical analysis was conducted and mechanisms that can play a defining role in film cooling control were identified on the basis of fundamental fluid-dynamics, prior experiments and preliminary numerical simulations. A cold flow wind-tunnel experiment incorporating a scaled-up, single film-cooling jet on a flat wall with a 90° injection angle was designed and built. The theoretical analysis was used to identify a window of essential flow-modulation parameters (frequency, duty cycle, mean blowing ratio, blowing ratio amplitude) within which film-cooling flow performance is expected to improve. A flow-pulsing system was designed, built and dynamically characterized. Both the wind tunnel boundary layer and jet exit flows were characterized using constant temperature anemometry. A series of preliminary experiments were conducted using reactive, Mie-scattering, laser-sheet visualizations for three mean blowing ratios with nearly zero low blowing ratio in the cycle, two duty cycles and four pulsing frequencies. The visualization results indicate that for the transverse jet with 90° injection angle, low frequency pulsations of the jet flow tend to increase the lateral coverage of the jet relative to the benchmark steady case without causing substantial lift-off at a blowing ratio of 0.5 and duty cycle of 50%. The observations are encouraging as to the feasibility of controlling the film cooling jet through mass flow pulsation and are consistent with predictions from fundamental analysis in terms of anticipated favorable operating conditions.

<b>14. SUBJECT TERMS</b>		<b>15. NUMBER OF PAGES</b> 30
		<b>16. PRICE CODE</b>

<b>17. SECURITY CLASSIFICATION OF REPORT</b>	<b>18. SECURITY CLASSIFICATION OF THIS PAGE</b>	<b>19. SECURITY CLASSIFICATION OF ABSTRACT</b>	<b>20. LIMITATION OF ABSTRACT</b>

## Project Task and Objectives Table

#	Task Description	Schedule
1.	Completion of fabrication and assembly of the mass-flow modulation system for the film-cooling jet	Completed
2.	Wind Tunnel boundary layer characterization with/without film cooling jet (X-Wire) Exit-Plane velocity survey of un-modulated film-cooling jet in cross-flow (X-Wire) <u>Conditions:</u> Density Ratio=1, Injection Angle=90°, Compound Angle=0°, Blowing Ratios=0.5, 1, 1.5, X-flow Velocity=0.5-10m/s <u>Rational:</u> Need to define base-line conditions	Completed
3.	Mass-Flow Modulation System Identification – Exit-Plane time-resolved velocity survey (X-Wire), unsteady mass-flow measurement (Integrating Mass-Flow Meter) <u>Target Conditions:</u> Peak-to-peak blowing ratio amplitudes variable in the range 50%-100% of the mean, blowing-ratio duty cycles 25%, 50%, 75%, frequency range 0(0.5Hz-10Hz). <u>Rational:</u> Knowing the velocity distribution and signal at the exit of the jet and the time evolution of the flow-rate are essential to being able to draw conclusions from film-flow observations. Therefore, the relationship between the jet-exit velocity signal the flow-rate signal and the imposed waveform of flow modulation system valve opening and closing is necessary. Knowledge of the latter alone is of very limited use because it is strongly system-dependent. Frequency range is selected on the basis of integral time-scale of the x-flow.	Completed
4.	Investigate the effects of jet mass-flow modulation on the film flow (Laser-sheet reactive Mie-scattering Visualization using TiCl <sub>4</sub> ) <u>Conditions:</u> As stated in 2 and 3 above adjusted with feedback from observations. <u>Rational:</u> Visualization of the mixing regions using a reactive technique will allow qualitative assessment of the extent of jet penetration into the cross-flow, lateral jet spread, mixing of jet fluid with the cross-flow and potentially reveal unsteady organized structures of significance.	Completed
5.	Assessment and Report of Results	Completed

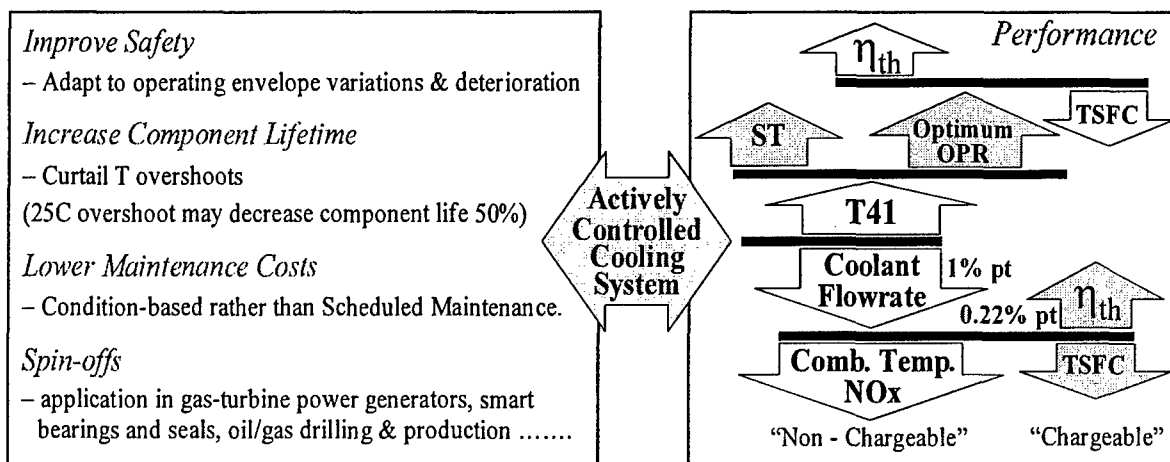
### Variations from original tasks:

Originally, blowing ratios 1, 1.5 and 2 were planned, but this was revised to 0.5, 1, 1.5 because under forced conditions an average blowing ratio of 2 would involve maximum blowing ratios during the forcing cycle that are excessively high. Furthermore, a blowing ratio of two is rather high considering that the film cooling jet for this study has an Injection Angle of 90° and no compound angle and is thus more prone to lift-off at such a blowing ratio.

Originally, forcing frequencies were anticipated in the range of 10-100Hz. The frequency range was determined on the basis of theoretical analysis, which is presented in this report and is dependent on free-stream velocity and boundary layer thickness among other variables. The chosen free stream velocity for the study was made after assessing the performance of the wind tunnel at the low end of its free stream velocity capabilities. It was found during task 2 that the quality of the flow (free-stream and boundary layer) was satisfactory at very low velocities. So, cross-flow conditions for the visualizations were picked so as to lower the forcing frequency by an order of magnitude thus matching the best performance envelope of the in-house developed forcing system.

## Motivation for the Project

The ability to substantially improve gas-turbine engine performance through passive means (e.g. geometry design) is approaching the point of diminishing returns. Revolutionary improvements in engine performance can be realized through introduction of intelligent systems. Numerous efforts are underway to develop actively controlled intelligent engine subsystems (inlet, compressor, combustor, jet nozzle), but very few in the turbine hot gas path. Application of active, local or global, control technology in the turbine has to overcome formidable challenges posed by the harsh environment, but can lead to substantial thermal management and/or aerodynamic performance increases.



ST – Specific Thrust  $T / \dot{m}_{air}$

OPR – Overall Pressure Ratio

$\eta_{th}$  – Thermal Efficiency

TSFC – Thrust Specific Fuel Consumption  $\dot{m}_{fuel} / T$

Figure 1: Benefits summary of Actively Controlled Cooling System

The potential benefits associated with an actively controlled cooling system are summarized in Figure 1. The resulting improved thermal management implies turbine inlet temperature (T41) increase and/or coolant economy without compromising turbine components. Increase of T41 can result into increased specific output (thrust or power depending on the application) or push the temperature-dependent optimum overall pressure ratio (OPR) to higher values yielding better efficiency. Considering that a substantial fraction (up to 30% for engines and 23% for power generators) of the compressor mass flow is diverted for cooling/purging purposes, coolant reduction can substantially benefit engine performance in terms of efficiency and/or emissions. Reduction of “chargeable” coolant (injected downstream of the 1<sup>st</sup> stage nozzle throat) will impact efficiency, while reduction of “non-chargeable” coolant will result in lower combustion temperatures and an associated NOx reduction. In addition to such performance

improvements, a robust active control technology will result into a cooling system able to optimally adapt to a varying operational envelope and may contribute to lifetime increases of hot-gas-path components by curtailing temperature overshoots. Benefits in reduced maintenance and safety can be substantial, considering that margins are very tight (e.g. a sustained maximum material temperature overshoot by as little as 25C may cut part life by 50%).

The following quotation from [1] justifies the effort and identifies the principal challenge regarding film-cooling control: "Noting the substantial amount of core flow required for cooling the turbine, and the substantial maintenance cost associated with the turbine, flow control technologies that improve the film cooling effectiveness would also be valuable. Since the goal is a layer of un-mixed cool air hugging the airfoil surface, a concept would be required to reduce, not enhance, mixing."

## **Background**

The effectiveness of a film-cooling system depends on the extent to which the cool jet-fluid adheres to the cooled component surface. Lift-off of the cooling jet flow and mechanisms promoting mixing, cause loss of cooling effectiveness and/or increase of heat-transfer as they allow hot "free-stream" fluid to come in contact with the component surface. In terms of the fluid mechanics of film cooling the objectives of an optimized film-cooling system are: minimization of jet lift-off, maximization of film coverage (i.e. large lateral jet/film spread, sustained film integrity downstream) and inhibition of mixing between the hot cross-flow stream and the cooling jet/film flow. In addition, it is important that the desired protection of the component surface is achieved with minimum use of the cool air resource and with minimal pressure loss.

It is not until recently that an initial investigation of the potential advantages of using active control of a film cooling flow to improve its performance has been conducted at AFRL-WPAFB [2]. In addition to this study, we will discuss a few relevant fundamental ones, a few applied ones that have pursued film-cooling performance improvements through passive means, and some relevant studies examining effects of flow unsteadiness in the cross flow on the film-cooling flow performance. The choice of these studies has been made on the basis of (a) insights they provide into flow mechanisms that can be affected through active control to improve film-cooling performance and/or (b) guidance regarding the means and methods.

Most studies of jets in cross flow (or transverse jets) to date, including two very useful fundamental ones by [3] and [4], have identified the counter-rotating vortex pair (CRVP), which forms inside the swept-back, film-cooling jet in cross-flow and is related to jet lift-off and increased entrainment

of cross-flow fluid underneath the film-cooling jet; both undesired effects for our application. These studies have related the roll-up of the jet shear layer to the initiation of the CRVP and, at higher blowing ratios, the separation of the flat-wall boundary layer leading to the formation of a wake vortex system beneath the downstream side of the jet. This wake vortex system also feeds into the CRVP and contributes to undesirable coolant mixing with the cross-flowing stream. Hence, it can be concluded that active control resulting into suppression of the CRVP, inhibition of the jet shear-layer vortex rollup and prevention of the boundary-layer separation events may fulfill the metrics of film-cooling performance detailed previously. Indeed, one of the cases studied by [4] has indicated that at high blowing ratios the jet lift-off was reduced when forcing of the transverse jet was applied. The experimental studies of [5] and [6] on transverse jets with tabs demonstrate how the transverse jet can be made to adhere better to the flat wall when triangular tabs are used on the upstream lip of the jet. In a more recent study [7] also demonstrated improvements in film cooling performance with upstream tabs. In these studies it is concluded that the improved behavior was caused by the generation of vorticity opposing, and therefore suppressing, the CRVP. Thus, one may conclude that improving the film-cooling flow can be achieved through actively controlling fluidic generation of such vorticity.

Many studies have been conducted exploring geometric (passive) modifications of film-cooling jets with the intent to improve film-cooling performance. These include the use of rectangular jet holes ([8]) compound angles ([9]; [10]) and shaped holes ([11]; [12]; and [13]). Almost all geometrical configurations that have resulted in film-cooling performance improvements have done so by effectively modifying the initial condition of the transverse jet(s). It is conceivable that similar modifications can be effected fluidically (through actuation). If so, the benefits can be realized over a broad spectrum of operating conditions through an active control system regulating the fluidic actuation with feedback from a performance-linked variable.

Studies of unsteady effects because of upstream turbine blades/vanes (e.g. [14, 15, 16], [17]; [18]) or large-scale unsteadiness originating from the combustor (e.g. [19]; [20]) also make a good case for the use of active film-cooling control. On one hand these studies demonstrate that periodic perturbations (though dictated by operational constraints and not targeting process control) can significantly influence the film cooling performance locally and globally, on the other hand the unsteady conditions are detrimental to film-cooling performance based on fixed (not adaptive) film-cooling operating conditions.

Recent studies have also revealed the importance of the geometry and flow that feeds the film cooling jets. The combined effect of film-cooling holes, internal cooling channels with rib turbulators and

bleed holes was discussed by [21] for smooth blades. Among several such studies, film-cooling measurements by [22] provide some very interesting insights by demonstrating a strong influence of the coolant inlet conditions on film cooling performance. This indicates that fluidic actuation applied in the internal cooling passages that feed the film-cooling flow can be used to control the film-cooling jet(s) performance. This is very important for the feasibility of active control applications in the hot gas path, because it allows actuator placement in a more protected (lower temperature, no contact with combustion products) environment, without compromising performance.

Based on the relevant prior work discussed above, it appears that good potential exists towards improving film-cooling by introducing fluidically (i.e. though flow excitation) characteristics and phenomena which have proven to be beneficial when introduced though passive means. In what follows we will examine and discuss two methods of exciting the film-cooling flow and attempt to identify windows of associated parameters, which are promising. We will draw upon the experience provided by the experimental study of [2] and our own computations.

## **Project Outcomes**

### ***Theoretical Analysis***

#### **Evaluation of Flow Excitation Methods**

In general there are two basic methods of exciting the flow that can and have been used in active flow control. The first method is to introduce simple or complex periodic excitation of a flow with small amplitude perturbations superposed on a steady mean flow, and rely on the complex non-linear dynamics between excited large-scale structure modes and the fine-grained turbulence in the flow to bring about the desired result, which most of the times has been the enhancement of mixing. This has been practically achieved acoustically and through other global or local actuation means. Typical examples of this strategy from among a plethora of studies in a broad variety of flows are those of [23] using global actuation, [24] using local actuation, [25] and [26] using acoustic actuation.

The second method is to modulate the flow rate itself at rather higher amplitudes in order to bring about the desired result by imposing the forcing signal as the dominant mode in the flow globally. This is the method employed in a jet in cross-flow for mixing enhancement studies by [27], [28] and the one recently used by [2] for film-cooling performance improvement.

#### **Complex Periodic Excitation**

We will examine evidence of the potential feasibility of both methods starting with the first one, using some non-linear stability simulation results from [29, 30]. They examined the response to complex periodic excitation of a laminar wall jet, which is a basic flow relevant to a class of film-cooling applications (particularly when using slots rather than holes). A schematic of the basic wall jet, velocity profile and terminology is shown in Figure 2.

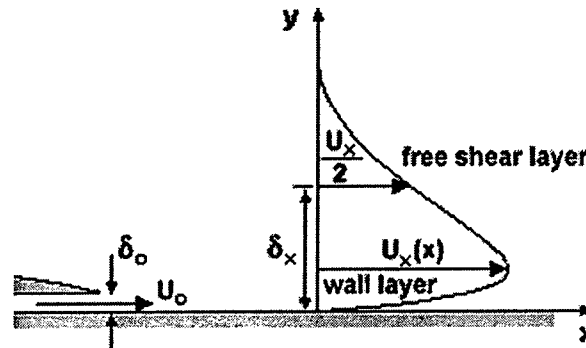


Figure 2: Typical mean velocity profile of film-cooling wall jet

In this study three spatially evolving large-scale vertical structures modeled as instability modes of the shear layer of the wall jet were forced at different energy levels and with prescribed initial phases in a similar manner as used by [31] for a plane mixing layer. The three modes forced were the natural (fundamental) frequency of the shear layer,  $f_n$ , its 1st subharmonic,  $f_n/2$  and its  $3f_n/2$  fractional harmonic. The coupled non-linear equations for the amplitudes and phases of the three modes and the mean-flow evolution equation derived through an integral energy formulation were solved subject to specific initial conditions.

Some time-averaged results of the simulation are portrayed in Figure 3 for three sets of modal initial conditions and the unperturbed flow labeled “no large-scale structures”. The initial energies of the three modes scaled by the initial kinetic energy of the mean flow are designated by,  $E_k$ , with  $k=1$  corresponding to  $f_n/2$ ,  $k=2$  to  $f_n$ , and  $k=3$  to  $3f_n/2$ , while the initial phases are designated by,  $\psi_k$ , with  $\psi_1=0$  (reference). In order to give a perspective of the forcing levels in realistic terms we mention that an initial modal energy of the order  $10^{-3}$  corresponds to a perturbation of 3.2% of the initial wall-jet mean velocity peak. The natural frequency ( $k=1$ ) in dimensionless form corresponds to a Stouhal number of approx.  $Str_{WJ}=0.16$  based on wall-jet maximum velocity and thickness. Figure 3 indicates that the downstream evolution of mean properties such as entrainment (representing extent of mixing with the free stream) and

skin friction coefficient (reflecting near wall transport) can be manipulated substantially through multimode modulation of wall jet instability modes. In this, the non-linear interactions between the instability modes play a key role as has been shown repeatedly by [31, 32] and [29, 30].

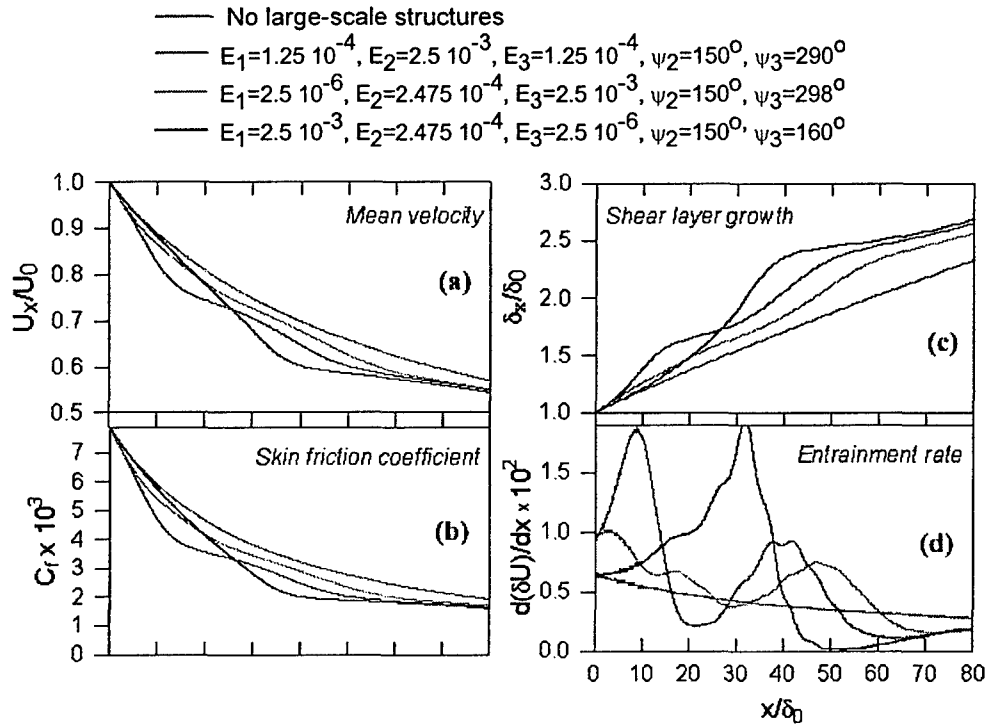


Figure 3: Effect of complex periodic forcing on evolution of wall-jet mean velocity (a), skin friction coefficient (b), thickness (c), and entrainment rate/mixing (d). (from [29]).

In order to aid the reader in interpreting Figure 3 we note that (i) faster growth of the wall-jet thickness (Figure 3c) is associated with growth and dominance of a large-scale vortical structure mode indicating either the first roll-up of vortices associated with the initially dominant mode or vortex merging ([23]), and (ii) this vortex action and the faster growth of the wall-jet thickness are also associated with entrainment peaks (Figure 3d), i.e. mixing enhancement, and the reduction of the peak wall-jet mean velocity (Figure 3a). So, looking at the entrainment in Figure 3d we see that mixing with the free stream can be enhanced or suppressed locally by factors as high as 3 to 4 relative to the un-perturbed flow. The second case from the top in the legend (red line) represents a transitional flow where the fundamental ( $k=2$ ) rolls up first resulting in the entrainment peak and associated fast growth of the wall-jet thickness in Figures 3d and 3c respectively around  $x/\delta=10$ . The sub-harmonic ( $k=1$ ) emerges naturally because it is

avored by non-linear interactions with other modes and the mean flow more so than other frequency modes. In this case the second entrainment peak in Figure 3d and thickness growth in Figure 3c are indicative of vortex merging associated with the sub-harmonic. From this perspective, the third case in the legend (green line) would represent successful suppression of entrainment (mixing) in a transitional wall-jet via dominant forcing of the fractional harmonic ( $k=3$ ). Likewise the fourth case from the top in the legend (blue line) represents significant enhancement of mixing in the near field resulting from the forcing of the sub-harmonic mode ( $k=1$ ). Finally, looking at the skin friction evolution of Figure 3b we find that it is generally reduced in the perturbed transitional flow relative to the laminar baseline and can be manipulated within a range of up to 40% by appropriately adjusting the forcing energies and phases between the three modes used in this numerical simulation.

The results of Figure 3, and invoking the momentum/heat transport analogy, indicate that mixing and near-wall heat transfer can be controlled in film-cooling flows through low-level, complex periodic forcing, at least in theory. The inclusion of small-scale turbulence effects will not significantly change this qualitative conclusion. However, from the practical perspective we note the following:

- (a) Practical implementation of low-level forcing of the film-cooling jet and controlling signal amplitudes and phases is very difficult. If it is applied locally, manufacturing and materials problems associated with embedding actuators become a significant challenge. If the actuation is effected in the larger coolant distribution conduits, which is quite feasible, it will be difficult to maintain the required character of the excitation at the coolant jet exit without knowledge of the associated transfer function and a feedback control system requiring embedded sensors, also a challenging undertaking. This approach is not irrevocably unfeasible in practice. Already there are examples in practice of embedding sensors such as thermocouples and strain gauges on vanes for testing purposes. However, improving their durability and developing actuators require significant research efforts and a long lead-time for practical and economic feasibility.
- (b) From the results in Figure 3 it is observed that low-level forcing in the range of the frequency spectrum around the natural frequency, say from its 1st subharmonic to its 1st harmonic (the high "amplification" range according to linear stability; [33]), although it most likely suppresses skin-friction (and by momentum/heat transfer analogy reduces near-wall heat transfer) it is also likely to favor mixing in the shear layer between the coolant jet and the hot stream. This makes it more risky because enhanced mixing may spell the destruction of the coolant film.
- (c) The natural frequencies of the shear layer separating the cool wall layer from the hot free stream can be quite high, of order of several hundreds of Hz at best and most likely of kHz. This poses an additional challenge of high frequency response on the actuators that may be necessary.

In view of these challenges low-level, complex periodic forcing of film-cooling flows may be risky in practice. The conclusions reached here were drawn from a wall-jet theoretical test-bed. One might

think that they may not apply to film-cooling flow emanating from round or elliptical holes. We maintain that the general conclusions still apply to this case considering that the blowing ratios typically used are low (at most of order 2) and that the initial jet flattens out over a short distance from its origin to resemble more a wall jet. This is more probably true since in most cases the injection is not normal to the protected wall surface through the use of non-zero compound angles (e.g. [2]) combined with injection angles less than  $90^\circ$ . Another point of doubt may be that the conclusions may not hold if the boundary layer in which the injection is effected is turbulent while the above analysis is based on a laminar flow. In general, even in the presence of local “backscatter”, fine-grained turbulence will be enhanced through forcing in the “amplification” range through non-linear interactions with the discrete modes, especially the higher frequency ones, which will on one hand tend to blunt their growth and survivability and on the other increase small scale mixing. So, the presence of small-scale turbulence can only make things worse if excitation is applied at frequencies in the “amplification” range, especially in the case of low-amplitude modulation.

#### High-amplitude Coolant Flow Modulation

The second approach to control film cooling involves high-amplitude modulation of the coolant flow-rate. In terms of potential practical implementation of this method, there is a principal concern regarding the application of high-amplitude pulsing. This concern is that the heavy valving involved may disrupt the coolant supply system and feed pressure pulses back to the compressor stages wherefrom the coolant is bled. This is a serious concern, but it can be addressed through the use of a valve that on each action simply redirects the flow of the coolant from one turbine blade stage to another. With this strategy the coolant flow path remains virtually undisturbed, especially if attention is paid to maintain the acoustic impedance of the two paths after the valve closely comparable.

The analysis of the previous section is still important in this case as well, because at higher forcing amplitudes non-linear spectral interactions become even more important with potentially similar consequences, especially if the forcing frequencies approach the neighborhood of the wall-jet natural

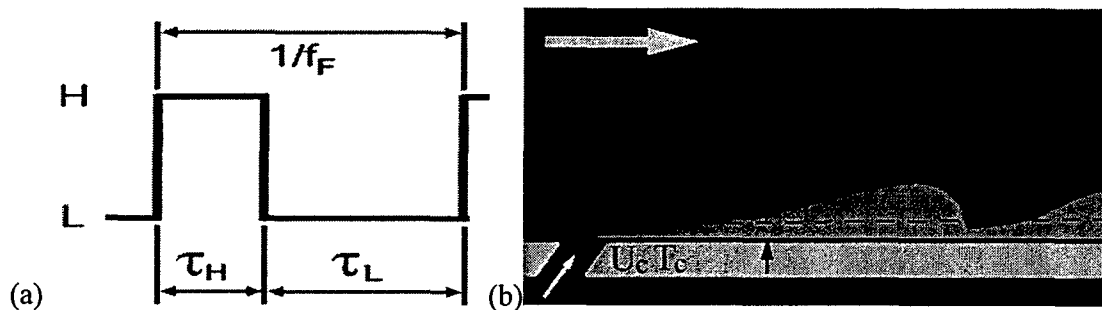


Figure 4: Cartoon of pulsed transverse jet and pulsing cycle with associated terminology.

frequencies (see "amplification" range in (b) above). So, it will be used as a guide in potentially recognizing a range of frequencies to be avoided, at least during a first-order effort. Much higher frequencies than the above-mentioned range are both less practically feasible and will have shorter range and lifetimes due to reduced potential of drawing energy from the mean flow and higher energy drain from small-scale turbulence, especially if the boundary layer and wall-jet are turbulent to begin with (see for example [34]). This leads to the conclusion that the most likely beneficial range of frequencies for large-amplitude coolant jet modulation should be well below the wall-jet natural mode.

The above statement is reinforced by the work of [2]. They were the first to report the pursuit and achievement of film-cooling performance improvements through active control experimentally. Their approach was to modulate (pulse) the coolant mass-flow rate predominantly at low frequencies  $O(10\text{Hz})$  while the wall-jet mode corresponding to their conditions is of  $O(100\text{Hz})$ . In a series of warm experiments using infrared thermography, they examined the effect of pulsing frequency and duty cycle for various blowing ratios on film-cooling effectiveness and Frossling number ( $Nu/Re^{0.5}$ ) downstream of the film-cooling hole. Their test bed was a single film-cooling hole located above the stagnation point on a semi-cylindrical leading edge. The film-cooling hole had an injection angle of  $20^\circ$  and a compound angle of  $90^\circ$ . The smallest dimension of its elliptical exit profile was substantially larger than the laminar boundary layer. It should be noted that the duty cycles in [2] were based on valve actuation timing (open vs. closed) and probably do not reflect the exact duty cycles at the film-cooling hole exit. In addition, the spatial and temporal shapes of the jet exit profiles are not known for their experiments, and therefore it is highly possible that the "closed" condition based on valving does not imply a zero minimum exit velocity. This of course depends on the acoustic impedance of the actuation and transmission system used in its totality, which is also unknown. Although these details are important, they should not invalidate the conclusions of the order-of-magnitude analysis that follows.

Let us consider a single period ( $1/f$ ; where  $f$  is the pulsing frequency) of the expected velocity cycle at the exit of the pulsed film-cooling jet, which is schematically portrayed in Figure 4a. Following the traditional representation, this period is split into two time increments  $\tau_H$  and  $\tau_L$  corresponding to the time during which the jet injection velocity remains high (H) and low (L) respectively. How high and how low the velocity gets depends on the effective blowing ratio and the peak-to-peak variation, which are also parameters of importance. In interpreting the results of [2] we assume that during the low part of the cycle, the velocity (and blowing ratio) is not exactly zero but quite low. This is not unreasonable because, considering the low frequencies used in their experiments, if the exit velocity of the coolant jet was zero,

the coolant film would have disintegrated, mixed and washed off leaving the surface exposed for a relatively long time (especially for duty cycles less than 0.5). Consequently, degradation of film cooling effectiveness and/or heat transfer augmentation would have been observed more often, which is not the case. The term “long time” is put in perspective of the convective time scales, which are of order less than milliseconds compared to valve-off timescales of the order of tens of milliseconds at least. What reinforces this assumption is the fact that [2] *did* observe severe film effectiveness degradation at the 10% duty cycle. When the duty cycle is this low, it is more likely that the exit velocity will have enough time to indeed be reduced to zero.

It is well known that if the magnitude of the blowing ratio (BR) is high enough for the jet to “lift off” separation will form “behind” the jet, which is detrimental. If the BR is too low the coolant will adhere to the surface but will be quickly overwhelmed through viscous mixing (if BL is laminar) and/or conduction, or turbulent mixing (if BL is turbulent or transitional). It is reasonable to assume that these constraints on the blowing ratio apply to its values during the high and low parts of the pulsing cycle. So, the target blowing ratio extrema range should be between approximately 0.2 and 2, although these limits will depend on geometry (e.g. injection and compound angles) as well as the duty cycle and frequency.

The duration of the low part of the cycle should depend on the amount of time necessary for the coolant film remaining near the wall to disintegrate. If the next pulse that will inject higher momentum coolant is activated within that time-scale, then the burst of coolant will be able to overlap (because of its higher velocity) the thin coolant film created during the low part of the cycle and “protect” it as illustrated in the cartoon of Figure 4b. This mechanism is aided by the dynamics of a starting vortex created in the beginning of the high pulsing cycle, which we will discuss later with the aid of some computational results. The necessity of this “overlap” provides a basis to estimate a reasonable value for  $\tau_L$ . This time estimate should come from the relevant scale associated with the mechanism responsible for the destruction of the thin film. If the BL is laminar, the mechanism ought to be diffusion and the associated time-scale,  $\delta_f^2/\nu$ . If it is turbulent, the mechanism ought to be turbulent transport and the associated time-scale should be of the order of the “large” eddy turnover time,  $\delta_f/u'$ . The thickness of the film between pulses is designated as,  $\delta_f$ , and it is assumed that it will be at least of the order of the BL thickness at the film-cooling hole location since any coolant beyond that will have been convected away rapidly by the free stream. It is understood that there is substantial variability in  $\delta_f$  during this unsteady injection process but it is sufficient to use the value corresponding to the hole location under steady conditions for an order of magnitude estimate. In the case of [2] the boundary layer was laminar and its thickness is estimated to

be approx. 0.78mm; much smaller than the smallest dimension of the film cooling hole. Thus, the order-of-magnitude maximum estimate of  $\tau_L$  yields values of the order of a few tens of milliseconds. The estimate of the corresponding minimum pulsing frequency using the simple formula resulting from the definition of the duty cycle (DC) is:

$$f_f = (1 - DC) / \tau_L \quad (1)$$

This formula yields low bounds for the pulsing frequency of the order of  $O(10\text{Hz})$  increasing with decreasing DC. This is definitely of the same order of magnitude as the frequencies used by [2], which displayed improved film-cooling performance.

The preceding analysis provided a basis to estimate a lower bound of forcing frequency. Reasoning has already been presented in the previous section, under the discussion of low-amplitude forcing in the "amplification" range of the wall-jet shear layer, pointing to an upper frequency limit well below (e.g. half an order of magnitude) the wall-jet natural frequency. This can be reinforced with arguments that are more relevant to injection through round/elliptical holes and also apply to the near field of the film-cooling hole, which we did not cover previously. One of the potential reasons for obtaining better performance from pulsed coolant flow may be due to the disruption in the formation of the Counter Rotating Vortex Pair (CRVP), which needs to be fed by high blowing ratios and the resulting strong streamline curvature to survive. An other potential reason is that with pulsed coolant flow the horseshoe vortex system, which usually forms immediately upstream of the hole and bends around it, is disrupted and not given time to be established. This is important since the stream wise vorticity of the swept-back horseshoe vortex plays a significant role in entraining hot fluid under the jet coverage from the sides. If the pulsation becomes too fast, the high momentum puffs would come in closer succession. Thus they would be able to interact and connect the stream wise vorticity, which is the forming identity of the CRVP and provide enough time (in an integral sense) for the horseshoe vortex system to sustain itself. A similar argument can be made regarding the establishment of separation in the rear of the jet during the high part of the cycle. The discussion regarding the CRVP and the horse-shoe vortex viability can also be used as an argument to support keeping the maximum DC on the low side rather than the high side, say in the neighborhood of  $DC \sim 0.5$ . Of course this upper limit will depend on blowing ratio. Regarding a lower limit for the DC, it is reasonable to assume that for a fixed average blowing ratio reducing DC by too much may not allow injection of enough high momentum coolant to cover and protect the thin film remaining from the low-part of the cycle. Furthermore, especially at higher effective blowing ratios, the jet during a shorter high-part of the cycle may be too strong and may cause a strong separation behind the

jet, which will destroy the remaining film from the low-part of the cycle before diffusion (BL laminar) or turbulent transport (turbulent or transitional BL) can destroy it.

With these arguments reinforced by the results of [2] duty cycles in the range 0.25 to 0.5 approx. should define a feasible window of investigation, with frequencies in the range dictated by the simple formula (1) as a low bound, and less than half an order of magnitude of the wall-jet natural frequency as an upper bound.

#### The Role of the Starting Vortex

In order to examine in more detail the physics of pulsed film-cooling a numerical simulation has been performed for a transitional film-cooling jet injected at 25 degrees (from the horizontal) on a flat wall without compound angle. The domain included a coolant delivery-tube ( $L/D=5$ ) with specified boundary conditions at its inlet and adiabatic walls. Monotonically Integrated Large Eddy Simulation (MILES) was performed with TVD-corrected sixth order differencing schemes ([35]). The jet was modulated with a square-wave pulse such as the one illustrated in Figure 4a for the worst-case scenario where the low (L) BR is zero. The high (H) BR based on average jet-exit velocity normal to the surface and the maximum cross flow velocity is 1.5. Cases with three duty cycles (0.25,0.5,0.75) and various Strouhal numbers (based on the maximum cross flow velocity and jet-hole diameter) were calculated. Statistics are collected over a time period at which the flow would convect  $500D$  based on the maximum cross-flow inlet velocity. The calculations were done with 2 million grid points and shown to be grid independent. The present calculation results are primarily used to illustrate mechanisms important to pulsed film-cooling flow and secondly to illustrate the potential effect on film-cooling effectiveness. Similar calculations with a constant temperature condition will be necessary in the future in order to assess the effects on heat transfer rates and provide the definitive picture of potential outcomes.

A calculated time evolution (frames numbered 1-10) of the temperature field on the plane of symmetry of the film-cooling jet is depicted on Figure 5 from the beginning and through the end of the high blowing-ratio (BR) part of a cycle with  $DC=0.25$  and excitation at a  $Str=0.16$ . Note that the Strouhal number based on residual film thickness is at least an order of magnitude lower and well below the one corresponding to the wall-jet mode. The formation of the starting vortex ring at the exit of the jet hole in the beginning of the cycle is evident in Figure 5(1). Figure 6 serves as an aid to explaining the evolution of this vortex ring downstream by using vortex filament rings as a model. This evolution is very important in securing "protection" of the residual film from the low part of the cycle as described in the previous section. The vortex ring at its genesis is indicated in both Figures 5(1) and 6 as A and it is exposed to the

wall-normal velocity gradient and the associated span-wise vorticity, which is clock-wise; i.e. the top of the vortex ring is exposed to higher cross-stream velocity than the lower part. This causes the starting vortex ring to rotate clock-wise (B in Figures 5(2-3) and 6), stretch at the same time in the stream wise direction (C in Figures 5(4-7) and 6) and ultimately face the wall (D in Figures 5(8-10) and 6) covering the residual coolant film on the wall.

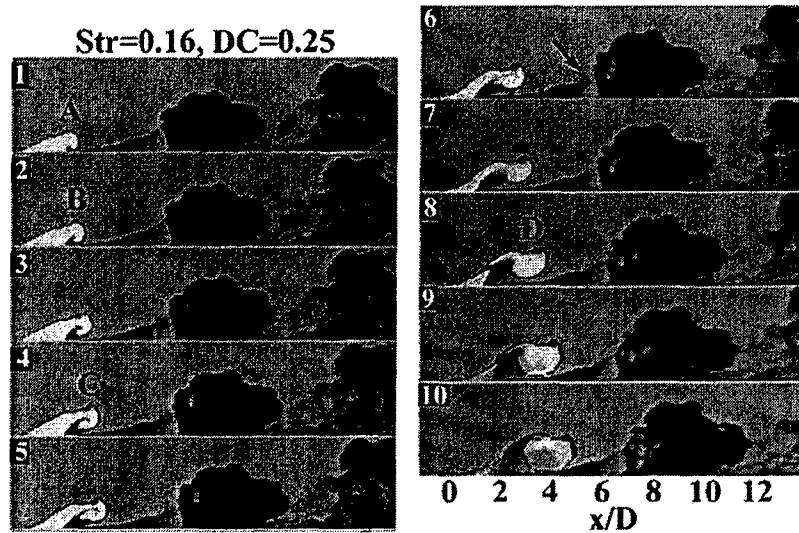


Figure 5: Sequence of time-steps from a numerical simulation of a pulsed transverse jet with a maximum blowing ratio of 1.5 and minimum of zero (color scale is inverted for better definition: i.e. coolant indicated by hotter colors).

It should be noted here that this behavior occurs as long as the starting vortex is not injected by an excessively high blowing ratio entirely into the free stream as in the case of [27] and [28]. In such case the dynamics are substantially different and the starting vortex does not turn and approach the wall. What is responsible for this behavior, apart from the near wall velocity gradient which initiates the process, are the induction phenomena associated with the mirror image of the vortex ring at each instant (indicated by lighter color in Figure 6). It can be shown that the rotation of the vortex ring is augmented by induction interaction with its mirror image on a purely inviscid basis. Furthermore, as the vortex ring is stretched in the stream wise direction, its curvature at both ends increases. This potentially introduces a self-induced velocity ([36]) in the neighborhood of the high curvature, which is normal to the local curved vortex filament plane and contributes to moving it towards the wall (see D in Figure 6). Finally, as the vortex ring stretches because of the strain rates in the BL, its sides resemble trailing vortices, similar to those in the wash of an aircraft.

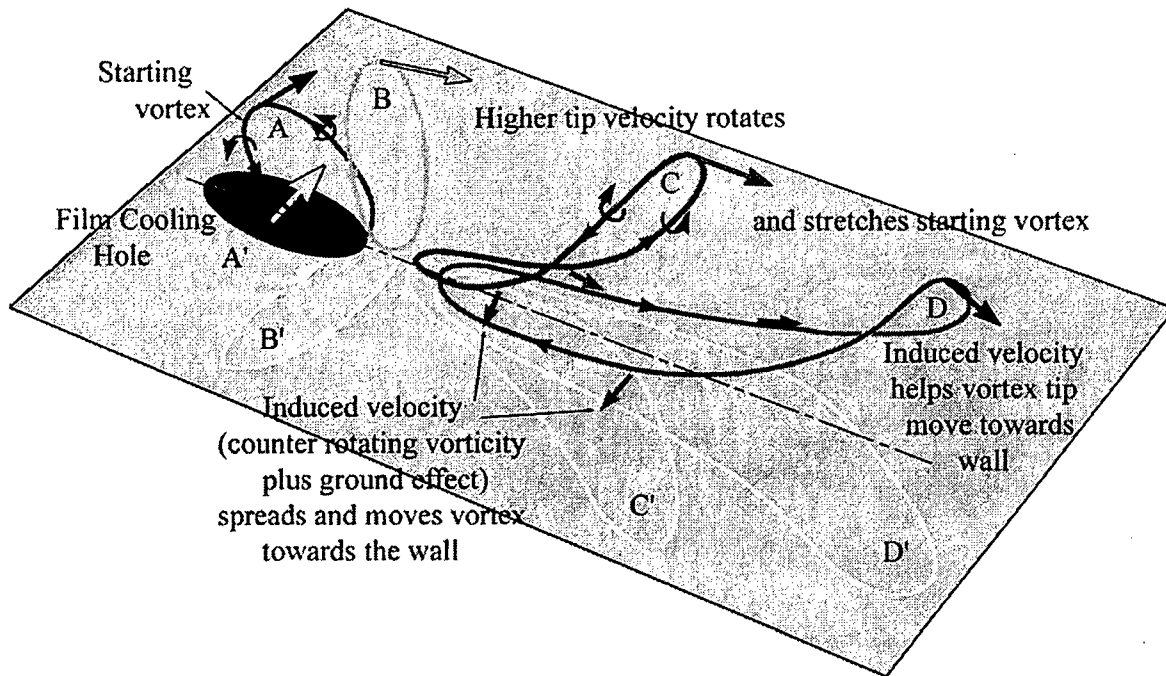


Figure 6: Schematic depictions of the near-field evolution of the starting vortex ring in a pulsed film-cooling jet. The mirror images of the starting vortex ring are in lighter color.

The induction interaction with the mirror image of the trailing vortices (commonly known as the ground effect) results in moving the side-branches towards the wall and in opposite span-wise directions as indicated by the colored side-arrows in Figure 6. It is this induction that ultimately helps the rotated and deformed starting vortex to move onto the wall and spread on to it, which is very beneficial to sustaining film coverage. This is indicated by the more dilute cool “puff” downstream of the starting vortex highlighted in Figure 5, which is the product of the starting vortex from the previous cycle.

It should also be noted that the vorticity direction on the side branches of the turned starting vortex is opposite to that of the CRVP, which is in the process of development so long as coolant is injected during the high part of the cycle. This could be significant because the opposing vorticity of the turned starting vortex can inhibit the formation of the CRVP, which has been shown to be effective by passive means as discussed in the introduction ([5], 1997; [6]; [7]).

Figure 5 also illustrates the point made in the previous section about the need to adjust the maximum and minimum blowing ratios in the cycle in order to avoid separation. In the case depicted in Figure 5 a separation bubble, indicated by the black arrow in Figure 5(6), indeed occurs during the peak

of the cycle. This separation bubble is convected downstream behind the starting vortex and eventually gets mixed in with it and the residual film. The identity of this separation bubble is also shaped by the fact that the starting vortex detaches itself from the jet during the injection part of the cycle as shown in Figure 5(8-10). This indicates that the time scale of starting vortex formation studied by [37] needs to be factored into the pulsed injection-timing scheme to avoid separation of the starting vortex from the feeding jet during the injection cycle.

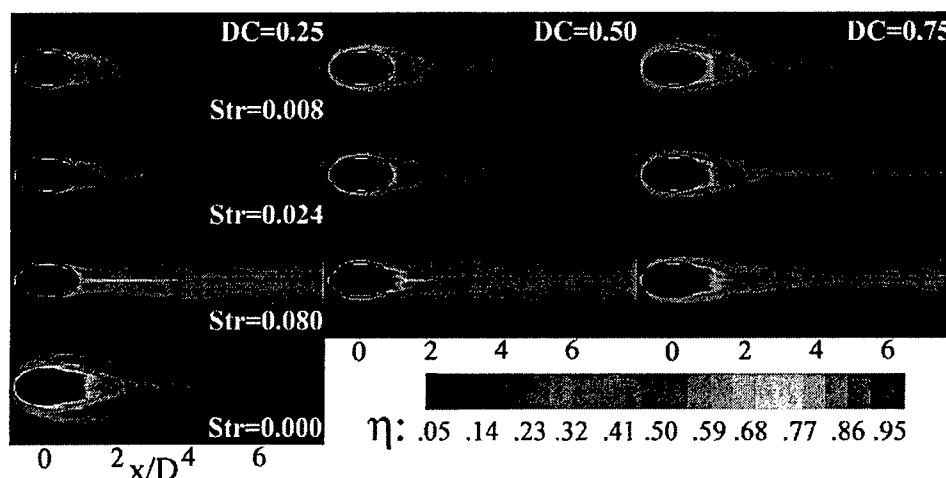


Figure 7: Effect of pulsing frequency (Str) and duty cycle (DC) on cooling effectiveness.

#### Time-Averaged Film-Cooling Effectiveness

Because of the adiabatic boundary condition only film-cooling effectiveness results can be obtained on the “cooled” surface, so potential benefits of pulsed film cooling can be presently discussed only with respect to this metric. The potential benefit of pulsed injection on film cooling is illustrated in Figure 7, which shows temporally averaged film cooling effectiveness contour plots for various cases simulated for this transitional film-cooling flow case. A Strouhal number (based on the maximum cross flow velocity and jet-hole diameter) of  $Str=0.08$  and duty cycles of 0.5 or 0.25 apparently provide significant enhancement in film cooling effectiveness over the unforced baseline case ( $Str=0$ ,  $DC=1$ ). It is worthy pointing out that at the lower frequencies (Str) there is evidence of increasing strength of the horse-shoe vortex around the leading edge and sides of the film cooling hole with increasing duty cycle. As explained in a previous section, this occurs because at high duty cycles the horseshoe vortex has more time to develop and maintain its coherence through the low part of the cycle. The effect is more pronounced at lower frequencies because again the time available for the horseshoe vortex to establish

itself is prolonged. Note also, that the presence of the horseshoe vortex is beneficial to the effectiveness around the hole, but, although its effect cannot be separated out in Figure 7, it is known from past experience to be detrimental in the rear of the jet. We also point out that the results of Figure 8 indeed show as explained previously (a) that high DC ( $>0.5$  here) reduces performance in terms of effectiveness at all frequencies, (b) that there is a lower limit in DC for good performance (note the reduction of effectiveness improvement at  $DC=0.25$  for most Str), and (c) that a lower-limit for the forcing frequency (Str) exists. It remains to be seen if an upper limit also exists as argued previously.

### **Experiments**

The experimental effort of this small project was directed towards designing and characterizing a cold-flow experiment which will serve as a vehicle to improve the understanding of phenomena associated with pulsed film-cooling flow and their potential effect on its performance. The experiment was developed and implemented in the LSU Wind Tunnel Laboratory. The experimental objectives of the project included characterizations of the wind-tunnel and "film-cooling" jet-exit flows and the low-frequency excitation system, followed by exploratory visualizations of forced and unforced transverse jet flows. All the characterizations were conducted through Constant Temperature Anemometry (CTA) hot-wire sensors manufactured by TSI appropriately calibrated in an automated calibration facility. Sampling conditions were chosen so as to ensure statistical independence of averaged quantities, acceptably low statistical uncertainty (e.g. less than 1% of the mean) and frequency spectra free of aliasing with good frequency resolution. To this effect integral timescales were determined using autocorrelation analysis prior to selecting the sampling conditions for mean quantities, and the Nyquist frequency of the acquisition was kept approximately an order of magnitude higher than the expected Nyquist frequency of the flow measured. A de-aliasing filter was always used with a cut-off frequency set lower than the acquisition Nyquist frequency.

A schematic of the test section used for the preliminary cold-flow experiments of this small project is shown in Figure 3 with associated flow nomenclature. The test section of the wind tunnel was 92 cm wide and 61 cm tall, while its useful length was approximately 3m. The wind tunnel test section is constructed so as to maintain a zero stream wise pressure gradient. The jet diameter was  $D=25\text{mm}$  and its center located at  $L_D=84\text{cm}$  from the beginning of the test section. The injection angle was  $\theta=90^\circ$ , and thus the compound angle,  $\alpha$ , was irrelevant. It is noted that the coupling between the jet system and the wind tunnel floor was designed so that it can be easily adapted to produce a jet with injection angles as low as  $30^\circ$  and continuously varying compound angles of up to  $\pm 90^\circ$ . The chosen injection angle constitutes a

“worst-case” scenario regarding the ability of the jet in cross flow to resist lift-off and tolerate relatively high blowing ratios under steady operating conditions.

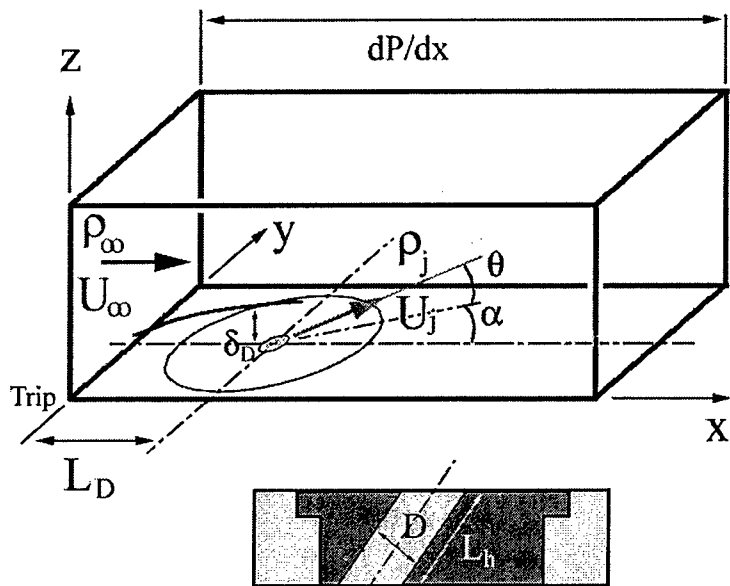


Figure 3: Schematic of the transverse-jet, wind-tunnel test section.

The wind tunnel free stream and boundary layer was characterized using single and X-wire constant temperature anemometry (CTA) probes for free stream velocities in the range of 0.5m/s to 10m/s. The objective of this characterization was to determine free-stream and boundary layer quality at low speeds. Low speeds are desirable because they lead to larger flow timescales (lower frequencies), and thus reduce the frequency response burden on the forcing system. The characterization of the boundary layer involved conducting detailed wall-normal ( $z$ -axis) surveys at nine different locations including the jet central plane ( $x$ - $z$ ), two planes symmetrical about this central plane in the span-wise direction ( $y$ -axis) at distances  $\pm 4D_j$  from the jet center plane and two cross-flow ( $y$ - $z$ ) planes one upstream ( $-4.75D_j$ ) and the other downstream ( $4.75D_j$ ) of the jet center. This was done in order to assess flow uniformity and integrity, turbulence levels in the free stream and velocity/turbulence profiles in the boundary layer, as well as spectral characteristics and timescales.

A sampling of boundary layer profiles from these characterizations demonstrating span wise uniformity at the stream wise location of the jet center is shown in Figure 4. The free stream was found to be uniform to within less than 1% at all locations. The turbulence level in the free stream was found to range from 0.2% at the lowest speed and not more than 0.5% at the highest speed tested, while no

significant discrete frequencies were found in the velocity spectra. This indicates that the soundproofing of the wind tunnel was successful and interference from acoustic frequencies is not an issue. On the basis of these characterizations a free-stream velocity of  $U_\infty=1.6\text{m/s}$  was chosen for the tests. At this free stream velocity the boundary layer at the jet location ( $L_D=84\text{cm}$ ) is laminar ( $Re_\delta=455$ ), which is the intended state for this study, with measured shape factor of 2.46 (2.59 theoretical). It is noted that the boundary layer in the case of [2] was also laminar, which was what motivated this as the initial choice. Under these conditions the mechanism responsible for film destruction is primarily viscous and the associated time scales provide a low pulsing frequency bound of less than 0.1Hz, while the BL integral time scale corresponds to frequencies around 450Hz and the convective jet time scales give frequencies of order 30-90Hz depending on blowing ratio. Thus jet-column mode instability without the effect of cross-flow would be in the range of 7-23Hz.

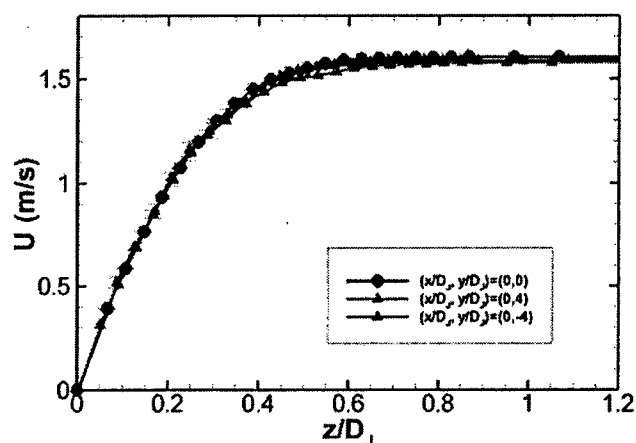


Figure 4: Boundary layer profiles at the jet span-wise center plane ( $yz$ ).

A similar survey was carried out also using CTA at the jet exit plane in order to assess the quality of the flow produced. This was done with all the auxiliary systems (forcing system and seeding systems for the visualizations) in place. Velocity surveys were performed on two orthogonal jet center plains ( $xz$  and  $yz$ ) at the exit of the jet ( $z/D_j=0.067$ ) for jet velocities corresponding to mean blowing ratios  $BR_m=0.5, 1, \text{ and } 1.5$  with respect to the chosen free stream velocity indicated previously. This was done under unforced conditions and without the cross-flow. At the test speeds of interest the corresponding jet  $Re$  numbers were approximately 1700, 3400 and 5100 respectively. Thus inside the jet tube the flow is laminar for the lowest blowing ratio and low- $Re$  turbulent for the other two blowing ratios.

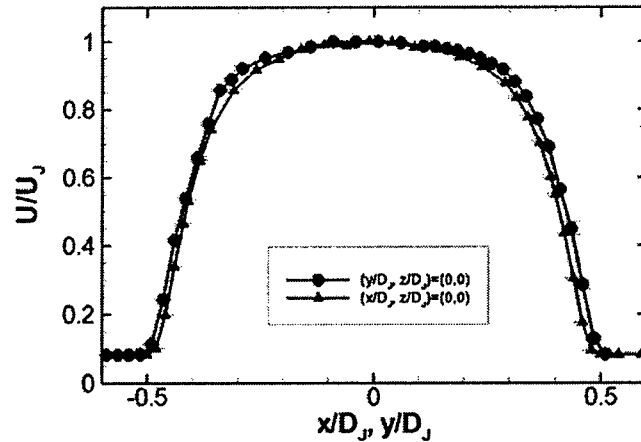


Figure 5: Jet-exit mean velocity profile without cross-flow for jet  $Re_j=3400$  corresponding to a mean blowing ratio of  $BRm=1$

Representative jet-exit velocity and stream-wise turbulence profiles for the  $Re=3400$  ( $BRm=1$ ) case are shown in Figures 5 and 6 respectively. It was verified that the axisymmetry of the jet flow is very satisfactory for all planned blowing ratios as indicated by the typical results of Figures 5 and 6. The mean velocity profile at the exit of the jet indicates that the jet is a weak one since the jet-exit boundary layers are thick and the potential core limited. The stream wise component turbulence profiles shown in Figure 6 indicate that the flow at the exit of the jet is not quite fully developed pipe flow. Neither of these features are expected to be detrimental to the purposes of this study.

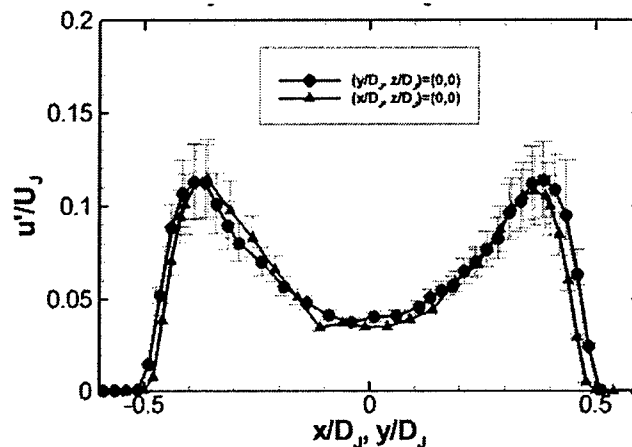


Figure 6: Jet-exit RMS velocity fluctuation profile without cross-flow for jet  $Re_j=3400$  corresponding to a mean blowing ratio of  $BRm=1$

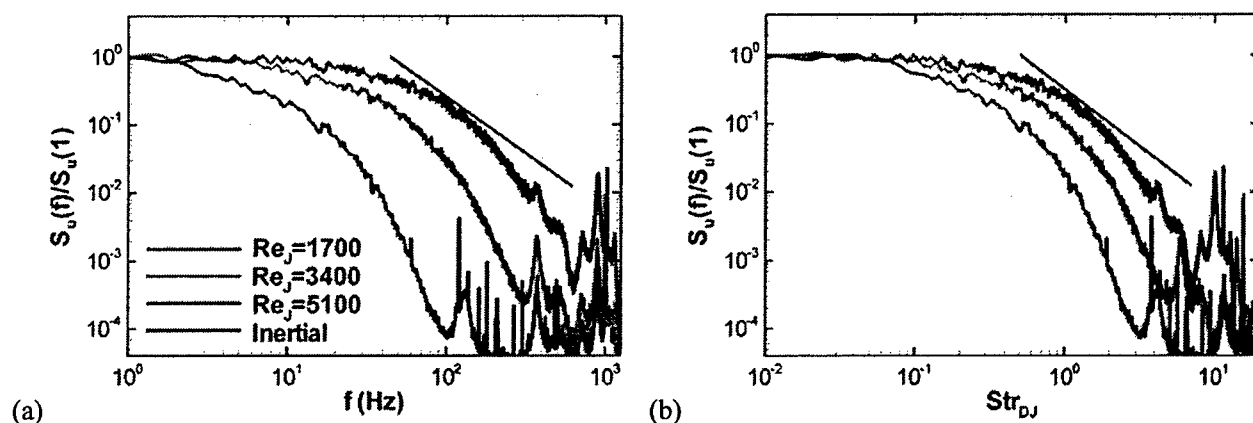


Figure 7: Velocity spectra from the center of the jet without cross flow corresponding to  $BRm=0.5, 1.0, 1.5$ . (a) Unscaled, (b) Scaled with jet convective time scale.

Velocity spectra, shown in Figure 7a, were obtained from the center of the jet exit and indicate that all frequencies induced by the jet air-supply system, forcing system and seeding system are at very low levels (at least an order of magnitude) relative to the energetic spectral band of the jet for all three operating speeds. In addition the majority of these frequencies are also higher than the jet cut-off frequency for all operating conditions and are therefore unlikely to be amplified through non-linear interactions with the jet spectral band. In Figure 7b the frequency is expressed as the jet Strouhal number (scaled with the jet convective time scale based on jet diameter,  $D_J$ , and jet centerline velocity,  $U_J$ ) and demonstrates that the low amplitude frequencies inherent to the jet system are far removed from the jet column mode amplification range of the jet which corresponds to Strouhal numbers of order  $10^{-1}$ . In these cases where the jet is weak with low ratio of the jet shear layer momentum thickness to diameter (e.g.  $2\theta/D_J=11$  for the  $Re_J=3400$ ) it is well known that the jet column mode preferred frequency coincides with the shear layer mode. Thus the jet shear layer amplification range is also well separated from the inherent system frequencies. Care was taken to design the jet air-supply, forcing and seeding systems so as to keep their acoustic frequencies outside the jet (and shear layer) spectral band, to avoid strong resonant interactions both under unforced and forced conditions. The straight lines in the graphs of Figure 7 indicate the  $-5/3$  inertial range spectral slope and it is evident from comparison with the three jet spectra, that only the one from the highest Reynolds number (5100) displays the traces of a forming inertial range, which is well known to fully establish itself at higher pipe Reynolds numbers than that.

A transient mass-flow meter with integration capability was used to measure the average flow rate during pulsed experiments. The pulsing parameter values to be investigated are peak-to-peak blowing

ratio amplitudes variable in the range 50%-100% of the mean, blowing-ratio duty cycles in the range 0.20 to 0.80, and a frequency range from 0.5Hz to 30Hz. These were selected on the basis of the theoretical rational discussed previously. Modulation of the film-cooling mass flow rate was applied through the use of a computer controlled mass-flow pulsing system, which was designed, built and fitted to the jet supply line. It incorporates two flow control valves and a single solenoid actuated valve. This system has the flexibility to adjust the high and low flow rates of the pulsing cycle at a fixed up-stream pressure and is capable of frequencies of up to 30Hz with variable duty cycle. The range of duty cycles achievable while preserving the integrity of the pulsing signature is dependent on the frequency of operation.

A static calibration of the mass flow modulation system was conducted in order to be able to predictably set the high and low flow rates (Blowing Ratio) in the pulsing cycle. As a result of the calibration a correlation was obtained between the relative positions of the two flow control valves and the magnitude of the velocity at the jet exit center. This was done at two different air supply pressures to cover both a low and a higher velocity range. Knowing the velocity distribution and signal at the exit of the jet and the time evolution of the flow-rate are essential to being able to draw conclusions from film-flow observations. Therefore, the relationship between the jet-exit velocity signal, the flow-rate signal and the imposed waveform of flow modulation system valve opening and closing is necessary. Knowledge of the latter alone is of very limited usefulness because conditions produced at the jet exit are strongly system-dependent. Therefore, proper system identification of the pulsing actuation system is critical to understanding the effects of the unsteady film-cooling flow on the flow phenomena that evolve in the cooling region downstream. Initial multipoint system identification was carried out over the exit plane of the film cooling jet. A typical single phase-averaged cycle of the jet velocity as measured at the center of the jet cross section on the exit plane is depicted in Figure 8. This was obtained by phase-averaging twenty pulsing cycles. The oscillations observed at the beginning of the high velocity part of the cycle are caused by a mechanical oscillation of the solenoid valve stem that occurs upon opening. The solenoid valve can be modified to deduce this effect. However, we conducted our initial tests without this modification in order to assess the sensitivity of the resulting pulsed film-cooling flow to such oscillations, which may appear in a practical implementation and are also documented by [38]. During the dynamic calibration it was concluded that the pulsing system performs well over the full desirable range of duty cycles (0.20-0.80) for frequencies up to 15Hz. At higher frequencies, the feasible duty-cycle range was limited to around 0.50.

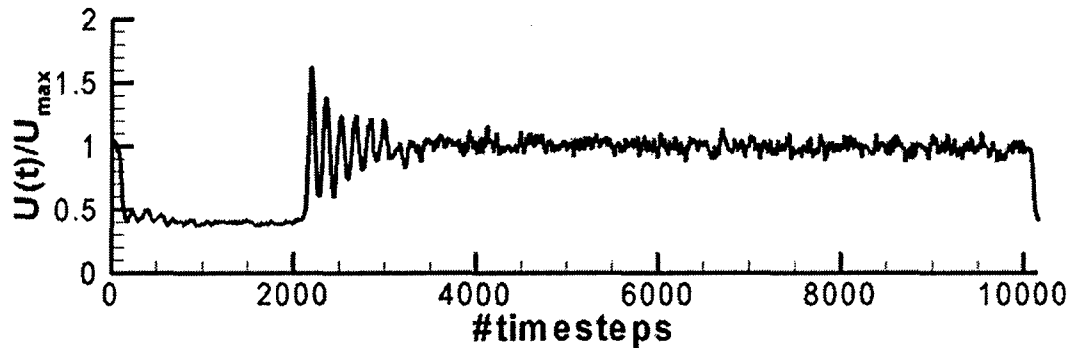


Figure 8: Sample of pulsed film-cooling jet velocity cycle measured at the center of the transverse jet exit. The forcing frequency was  $f_f=3\text{Hz}$ , and the target duty cycle was 80%.

The effects of jet mass-flow modulation on the film flow were investigated using laser-sheet reactive Mie-scattering visualizations using  $\text{TiCl}_4$ . To this effect a seeding system was designed and built. This seeding system uses dry air or nitrogen to entrain  $\text{TiCl}_4$  vapor into the stream of the jet where it reacts with moisture to produce micron/sub-micron-size  $\text{TiO}_2$  particles. The contribution of the seeding system to the flow rate of the jet was factored in during the dynamic calibration of the forcing system for pre-set seeding conditions.

Visualization experiments were conducted for three mean blowing ratios (BR<sub>m</sub>) of 0.5, 1 and 1.5 for duty cycles of 0.25, and 0.50 and for pulsing frequencies of 0.5Hz, 1Hz, 5Hz and 10Hz selected within the theoretical frequency range arrived at from theoretical considerations. In all these cases the lowest value of the blowing ratio was set by the seeding part of the flow and was of the order of  $10^{-1}$ . Visualizations were also conducted for the corresponding un-pulsed flows. They were all carried out on a horizontal (yx) plane at a level above the jet exit of the jet of  $z/D_j=0.56$ . While visualizations on a vertical plane would have been somewhat more revealing, these were not possible during the period of this study due to constraints the removal of which required modification of the automated traverse system, which is affixed at the top of the wind tunnel test section. Such modifications and visualizations on a vertical plane will be pursued during the continuation of this project. A New-Wave Nd-YAG laser emitting at 532nm wavelength and pulsed at 15Hz and 30Hz depending on the time-scale of the flow observed was used as the light source combined with variable-focus laser-sheet generating optics (combination of cylindrical and spherical lenses). A 1-Megapixel Megaplex black-and-white interlaced CCD camera fitted with a zoom video lens and synchronized with the laser was used to record the images. The external trigger signal for the laser-camera system was recorded along with the pulse train driving the flow forcing system. Thus the timing of the images relative to the flow pulsing cycle was known. This was achieved

through a National-Instruments data acquisition and relay board and an virtual instrument for Labview developed for the purposes of this project.

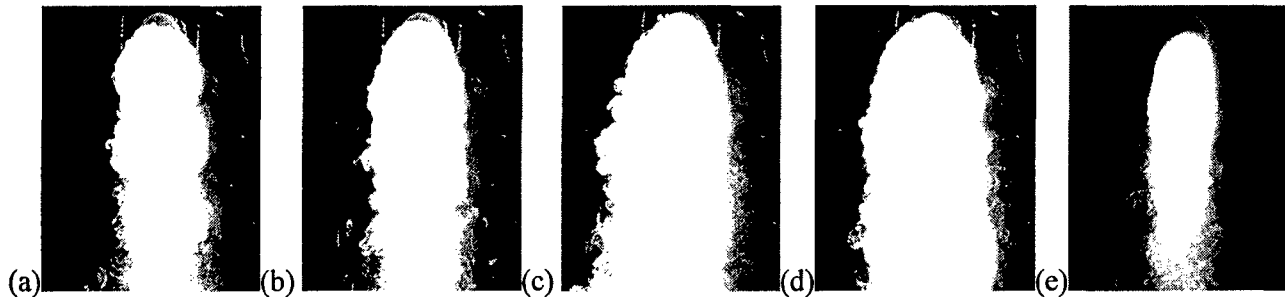


Figure 9: Time averaged (multiple-exposure) visualizations of the jet in cross-flow on a horizontal plane parallel to the wind-tunnel wall, at a distance of approximately  $0.56D_j$ .  $TiO_2$  smoke generated inside the jet tube seeded the jet. All flows were at  $U_\infty=1.6\text{m/s}$ , mean blowing ratio of  $BR_m=0.53$  and all forcing conducted at  $DC=0.5$  and peak-to-peak blowing ratio of approx.  $BR_{pp}=1$ . (a)  $f_f=10\text{Hz}$ , (b)  $f_f=5\text{Hz}$ , (c)  $f_f=1\text{Hz}$ , (d)  $f_f=0.5\text{Hz}$ , (e) Unforced

The visualizations at mean blowing ratios of 1 and 1.5 indicated that jet lift-off was occurring for all pulsed cases over the full range of the parameters attempted and the highest mean blowing ratio steady case, while jet lift-off was intermittent for the steady flow with blowing ratio of unity. This was not unexpected, considering the theoretical discussion in the previous section and because the jet injection angle used in the experiment constitutes the worst-case scenario in terms of propensity to lift-off. Indeed, during the high part of the cycle the maximum blowing ratio exceeds the value of 2, and as a result separation occurs behind the jet as described in the previously outlined theoretical analysis.

The visualization experiments at the lowest mean blowing ratio indicated that no sustained lift-off appeared and under certain conditions at a duty cycle of 0.5 the lateral spread of the jet increased significantly relative to the baseline steady flow case without sustained lift off. Time averaged (multiple-exposure) images indicating this are presented in Figure 9. It is evident that at pulsing frequencies of 0.5Hz (Figure 9d) and 1Hz (Figure 9c) significant increase of lateral spread occurs (by approx. a factor of 2) relative to the benchmark steady case. It is also observed that the jet is sustained at longer downstream distances than the benchmark steady case. The width of the field of view in the images of Figure 9 and subsequent images is approximately  $5D_j$ , while the length is approximately  $8D_j$ . Pulsing at the higher frequencies of 5Hz (Figure 9b) and 10Hz (Figure 9a) does not appear to offer as substantial an increase of the lateral spread of the jet. It should be noted that the increase of the lateral spread of the jet does not necessarily imply increased mixing and it is desirable in film cooling because it increases the protected

area of the surface. It is also noted that a frequency of 10Hz is inside the amplification range of the jet column mode instability and some degree of resonance with an amplified jet mode is expected.

The structural differences between the low-frequency pulsed case and the high-frequency pulsed case are better illustrated in Figures 10 and 11 where instantaneous visualizations are shown at various instances in the course of the duty cycle. It is observed that at the low frequency pulsation there is still some extent of coverage of the surface by  $\text{TiO}_2$ -particle-seeded jet fluid during the low end of the cycle during (Figure 10a and 10b) which, we remind the reader, the blowing ratio is very small but not zero. This tends to be in agreement with the analysis in the theoretical section of this report. There is no evidence of systematic or sustained separation behind the jet. During the high part of the cycle (Figure 10d and 10e) there is no evidence of jet lift-off and the lateral jet spread is substantial with evidence of large scale structure at a higher frequency than that of the pulsation (especially in Figure 10d). At the higher pulsing frequency of 10Hz the structure is quite different. Evidence of separation region can be seen created during the low part of the cycle between successive high-blowing ratio injections. This brings up an other consideration, which has not been covered by previous discussion. In the low pulsing frequency cases this separation also occurs but it occurs less often and it is relatively short lived because the low-blowing ratio part of the cycle has more time available to establish itself. In contrast when pulsing at a higher frequency the separation occurs more often. In addition, the shorter duration of the high-blowing-ratio part of the cycle does not release sufficient amount of jet fluid to laterally evolve promoting the encroachment of cross-flow fluid. In most of the instantaneous realizations of the beginning of the high-blowing ratio part of the cycle there is evidence of a starting vortex. However its dynamic behavior cannot be effectively observed through horizontal-plane visualizations.



Figure 10: Instantaneous visualizations of the jet in cross-flow on a horizontal plane parallel to the wind-tunnel wall, at a distance of approximately  $0.56D_j$ .  $\text{TiO}_2$  smoke generated inside the jet tube seeded the jet. All flows were at  $U_\infty=1.6\text{m/s}$ , mean blowing ratio of  $\text{BR}_m=0.53$  and all forcing conducted at  $\text{DC}=0.5$  and peak-to-peak blowing ratio of approx.  $\text{BR}_{pp}=1$ , and  $f_f=0.5\text{Hz}$ . (a),(b) during the low part of the cycle, (c) beginning of the high part of the cycle, (d),(e) during the high part of the cycle.

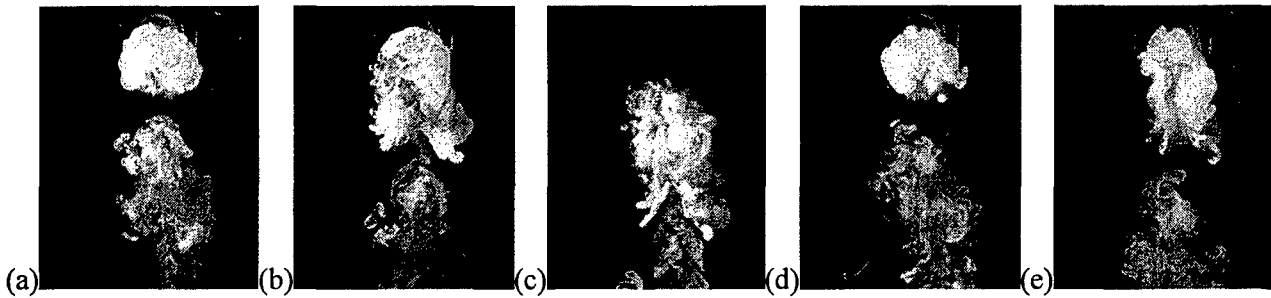


Figure 11: Instantaneous visualizations of the jet in cross-flow on a horizontal plane parallel to the wind-tunnel wall, at a distance of approximately  $0.56D_j$ . TiO<sub>2</sub> smoke generated inside the jet tube seeded the jet. All flows were at  $U_\infty=1.6\text{m/s}$ , mean blowing ratio of  $BR_m=0.53$  and all forcing conducted at  $DC=0.5$  and peak-to-peak blowing ratio of approx.  $BR_{pp}=1$ , and  $f_f=10\text{Hz}$ . (a) and (d) beginning of the high part of the cycle.

## Conclusions

In conclusion, from theoretical considerations we have presented an assessment of possible methods of excitation for the improvement of film cooling. Arguments have been presented on a theoretical basis that high-amplitude pulsing of the film cooling flow is a feasible method and identified a rationale and methodology for the choice of forcing parameter (blowing ratio, duty cycle, frequency) windows consistent with experiment ([2]). This rationale was partially verified through preliminary numerical simulation results. Furthermore, we have identified and discussed possibly important phenomena associated with pulsed film-cooling flow, such as the starting vortex and its role in the process. We have used the outcomes of the analysis as a basis for the design of a pulsed film-cooling experiment. This experiment has been set-up and the wind-tunnel experimental facility and pulsation system have been duly characterized. On the basis of this characterization, a cross-flow velocity was selected so as to make the characteristic timescales of the ensuing transverse jet flow compatible with the response characteristics of the pulsing system. Visualizations have been conducted for the worst-case scenario of a pulsed transverse jet with  $90^\circ$  injection angle at three different mean blowing ratios (0.5, 1, 1.5) with nearly zero low blowing ratio in the cycle, two different duty cycles (0.25, 0.5) within the range predicted as most likely to give positive results by the theoretical analysis and at four different pulsing frequencies (0.5Hz, 1Hz, 5Hz, 10Hz). The visualization results indicate that for the  $90^\circ$  injection angle transverse jet low frequency pulsations of the jet flow tend to increase the lateral coverage of the jet without causing substantial lift-off at the lowest mean blowing ratio and with a duty cycle of 0.5. The observations are encouraging as to the feasibility of controlling the film cooling jet through mass flow

rate modulation and are consistent with what is predicted by fundamental theoretical analysis in terms of anticipated favorable operating conditions. Thus the objectives of this limited scope project have been duly fulfilled and the foundation has been laid for further quantitative investigations of pulsed transverse jets as the means to improving film-cooling performance.

## Acknowledgment/Disclaimer

This work was sponsored (in part) by the Air Force Office of Scientific Research, USAF, under grant/contract number FA9550-05-1-0219. The views and conclusions contained herein are those of the authors and should not be interpreted as necessarily representing the official policies or endorsements, either expressed or implied, of the Air Force Office of Scientific Research or the U.S. Government.

## References

- [1] Lord, W. K., MacMartin, D. G., and Tillman, T. G., Flow Control Opportunities in Gas Turbine Engines, AIAA Paper 2000-2234, AIAA Fluids Conference, Denver, CO, 2000.
- [2] Ekkad, S. V., Ou, S., and Rivir, R. B., Effect of Jet Pulsation and Duty Cycle on Film Cooling from A Single Jet on a Leading Edge Model, IMECE2004-60466, ASME IMECE, Anaheim, CA, 2004
- [3] Fric, T. F. & Roshko, A. "Vortical structure in the wake of a transverse jet", J. Fluid Mech. 279, 1:47, 1994.
- [4] Kelso, R.M., Lim, T.T., Perry, A.E., An experimental study of round jets in cross-flow, J. of Fluid Mechanics, 306: 111-144, 1996
- [5] Zaman, K. B. M. Q., and Foss, J. K., The effect of vortex generators on a jet in a cross-flow, Physics of Fluids, 9(1), 109-114, 1997.
- [6] Zaman, K. B. M. Q., Reduction of Jet Penetration in a Cross-flow by using Tabs, Paper AIAA-98-3276, 34th AIAA Jet Propulsion Conference & Exhibit, Cleveland OH, July 13-15, 1998.
- [7] Nasir, H., Acharya, S., and Ekkad, S.V., "Improved Film Cooling From Cylindrical Angled Holes with Triangular Tabs: Effect of Tab Orientations", Intl. J. of Heat and Fluid Flow, Vol. 24, No. 5, 2003, pp. 657-668
- [8] Sivadas, V., Pani, B. S., Butefisch, K. A., Meier, G. E. A., Flow visualization studies on growth of area of deflected jets, Experiments in Fluids, 23 (2): 105-112, 1997
- [9] Nasir H, Ekkad SV, Acharya S, Effect of compound angle injection on flat surface film cooling with large streamwise injection angle, Experimental Thermal and Fluid Science, 25 (1-2): 23-29 AUG 2001
- [10] Goldstein, R. J., Jin, P., Film cooling downstream at a row of discrete holes with compound angle, J. of Turbomachinery, 123 (2): 222-230, 2001
- [11] Bell, C.M., Hamakawa, H., Ligrani, P.M., Film cooling from shaped holes, J. of Heat Transfer, 122(2): 224-232, 2000
- [12] Cho, H. H., Rhee, D. H., Kim, B. G., Enhancement of film cooling performance using a shaped film cooling hole with compound angle injection, JSME International Journal Series B-Fluids and Thermal Engineering, 44 (1): 99-110 FEB 2001
- [13] Lee, H. W., Park, J. J., Lee, J. S., Flow visualization and film cooling effectiveness measurements around shaped holes with compound angle orientations, International Journal of Heat and Mass Transfer, 45 (1): 145-156 JAN 2002
- [14] Bons, J. P.; Rivir, R. B.; Mac Arthur, C. D.; Pestian, D. J., The Effect Of Unsteadiness On Film Cooling Effectiveness, Wright Lab Report WL-TR-96-2096, 1996a.

- [15] Bons, J. P.; Rivir, R. B.; Mac Arthur, C. D., The Effect Of High Freestream Turbulence On Film Cooling Effectiveness, Wright Lab Report WL-TR-96-2097, 1996b.
- [16] Bons, J.P., MacArthur, C.D., and Rivir, R.B., The Effect of High Free-Stream Turbulence on Film Cooling Effectiveness, *J. of Turbomachinery*, 118, 814-825, 1996c.
- [17] Heidmann, J. D., Lucci, B. L., An experimental study of the effect of wake passing on turbine blade film cooling, *Journal of Turbomachinery*, 123 (2): 214-221, 2001
- [18] Teng, S. Y., Sohn, D. K., Han, J. C., Unsteady wake effect on film temperature and effectiveness distributions for a gas turbine blade, *J. of Turbomachinery*, 122 (2): 340-347, 2000.
- [19] Lee, J. S., Jung, I. S., Effect of bulk flow pulsations on film cooling with compound angle holes, *International Journal of Heat and Mass Transfer*, 45 (1): 113-123 JAN 2002
- [20] Jung, I.S., Lee, J.S., Ligrani, P.M., Effects of bulk flow pulsations on film cooling with compound angle holes: Heat transfer coefficient ratio and heat flux ratio, *Journal of Turbomachinery*, 124 (1): 142-151, 2002
- [21] Garg, V. K., Heat transfer research on gas turbine airfoils at NASA GRC, *International Journal of Heat and Fluid Flow*, 23 (2): 109-136, 2002
- [22] Wilfert, G., Wolff, S., Influence of internal flow on film cooling effectiveness, *J of Turbomachinery*, 122(2): 327-333, 2000
- [23] Ho, C.M. and Huang, L.S., Subharmonics and Vortex merging in Mixing layers, *J. of Fluid Mechanics*, 119: 443-473, 1982
- [24] Davis S. A. and Glezer, A., The manipulation of large- and small-scales in coaxial jets using synthetic jet actuators, AIAA-2000-0403, 38th AIAA Aerospace Sciences Meeting, January 10-13, Reno, NV, 2000.
- [25] Zhou, M.D., Heine, C. & Wygnanski, I. (1996), The effects of excitation on the coherent and random motion in a plane wall jet., *J. Fluid Mech.* 310, 1-37.
- [26] Choy, W.-H., Bonnafous S. and Nikitopoulos D. E., Forcing the Large-Scale Structures in Coaxial Jets, *Bulletin of the APS*, 46(10), 196; 54th Annual Meeting of the APS Division of Fluid Dynamics, San Diego, CA, Nov. 18-20, 2001.
- [27] Cortelezzi, L. and Karagozian, A. R., "On the formation of the counter-rotating vortex pair in transverse jets", *J. Fluid Mech.* (2001), vol. 446, pp. 347.
- [28] M'cLoskey, R.T., King, J.M., Cortelezzi, L. and Karagozian, A.R., The actively controlled jet in crossflow, *Journal of Fluid Mechanics*, 452:325-335, 2002
- [29] Morel S., and Nikitopoulos D. E., "Multiple Large-Scale Mode Interactions in a Laminar, Developing, Strong Wall Jet", *Bulletin of the American Physical Society*, Vol. 42, presented at the 50th Annual Meeting of the APS Division of Fluid Dynamics, San Francisco, CA, Nov. 23-25, 1997a.
- [30] Morel S. and Nikitopoulos D. E. "Non-Linear Interactions Between Two-Dimensional Wave-Modes in a Laminar Incompressible Wall Jet", LSU Report, LSU-ME-WALLJET-0002, September 1997b.
- [31] Nikitopoulos, D. E., and Liu, J. T. C., Nonlinear Three-Wave Interactions in a Developing Mixing Layer, *Physics of Fluids*, 13(4): 966-982, 2001.
- [32] Nikitopoulos D.E. and Liu J.T.C., "Non-Linear Coherent Mode Interactions and the Control of Shear Layers", in *Structure of Turbulence and Drag Reduction*, A. Gyr (Editor), Springer Verlag 1990.
- [33] Nikitopoulos D.E. and Liu J.T.C., "Nonlinear Binary-Mode Interactions in a Developing Mixing Layer", *Journal of Fluid Mechanics*, 179:345-370, 1987.
- [34] Liu, J. T. C., Large-Scale Coherent Structures in Free Shear Flows, *Appl. Mech. Reviews*, 1991
- [35] Muldoon, F., and Acharya, S., 2004, Direct Numerical Simulation of a Film Coolant Jet, ASME Intl. Gas Turbine Conference, Vienna, Austria, 2004, ASME-GT-2004-5350
- [36] Batchelor, G. K., "An Introduction to Fluid Dynamics", Cambridge Univ. Press (1979).

[37] Gharib, M., Rambod, E. and Shariff, K., "A universal time scale for vortex ring formation", J. Fluid Mech. (1998), vol. 360, pp. 121

[38] Ou S. and Rivir R. B., personal communication, summer 2005.

### **Personnel Supported During Duration of Grant**

Jeremiah Oertling	Graduate Student, LSU, Baton Rouge (AFOSR)
Pierre-Emmanuel Bouladoux	Graduate Student, LSU, Baton Rouge (AFOSR)
Dimitris E. Nikitopoulos	Professor, LSU, Baton Rouge (LSU Cost Share)
Sumanta Acharya	Professor, LSU, Baton Rouge (LSU Cost Share)

### **Publications**

"On Active Control of Film-Cooling Flows", D.E. Nikitopoulos, J. Oertling, S. Acharya and F. Muldoon, Paper GT2006-90051, ASME Turbo Expo 2006, May 8-11, 2006, Barcelona, Spain.

### **Honors & Awards Received**

None this reporting period

### **AFRL Point of Contact**

Richard Rivir, AFRL/PRTT, WPAFB, OH. Met at WPAFB on June 29, 2005.

### **Transitions**

None this reporting period

### **New Discoveries**

None this reporting period.